Advances in Physics Theories and Applications
ISSN 2224-719X (Paper) ISSN 2225-0638 (Online)
Vol.67, 2017
www.iiste.org

Heat and Mass Transfer in Radiative Casson Fluid Flow Caused by a Vertical Plate with Variable Magnetic Field Effect

R. Vijayaragavan* S. Karthikeyan
Department of Mathematics, Thiruvalluvar University,
Vellore-632 115, India

Abstract
The aim of the present study is to investigate influence of variable magnetic field, heat and mass transfer in radiative Casson fluid flow past an infinite vertical porous plate. The governing equations of the flow, heat and mass transfer are transformed into a system of nonlinear ordinary differential equations and solved analytically by the perturbation technique with matlab package. The results obtained show that the velocity, temperature and concentration fields are appreciably influenced by the chemical reaction, thermal stratification and magnetic field. It is observed that the thermal radiation and magnetic field decreases the velocity, temperature and concentration profiles. There is also considerable effects of magnetic field and chemical reaction on skin friction coefficient and Nusselt number.
Keywords: MHD, Variable magnetic field, Radiative, Casson fluid, dissipative, Heat transfer, Mass transfer.

Nomenclature

y : Dimensional distance along and perpendicular to the plate
g : Gravitational Acceleration
$\hat{T}$: Dimensional Temperature
T_∞ : Free stream dimensional Temperature
$\hat{K}$: Permeability of the porous medium
$\hat{C}$: Dimensional Concentration
C_∞ : Free stream dimensional Concentration
β_T , β_C : Thermal and Concentration expansion coefficient
$\hat{P}$: Pressure
C_p : Specific heat of constant pressure
μ : Viscosity
$\hat{q}_r$: Radiative heat flux
ρ , σ : Density and Magnetic Permeability
$\nu = \mu / \rho$: Kinematic viscosity
D , Q_0 : Molecular diffusivity and Dimensional heat
R : Chemical reaction
F : Magnetic Field

1.Introduction

Convective flow with simultaneous heat and mass transfer under the influence of a magnetic field and chemical reaction have attracted a considerable attention of researchers because such process exist in many branches of science and technology. Possible applications of this type of flow can be found in many industries viz. in the chemical industry, cooling nuclear reactors and magnetohydrodynamic (MHD) power generators. Free convection flow occurs frequently in nature. It occurs not only due to temperature difference, but also due to concentration difference or combination of these two. Many transport processes exit in industrial applications in which the simultaneous heat and mass transfer occur as a result of combined buoyancy effects of diffusion of chemical species. Free convection flows in a porous media with chemical reaction have wide applications in geothermal and oil reservoir engineering as well as in chemical reactors of porous structure. Moreover, considerable interest has been evinced in radiation interaction with convection and chemical reaction for heat and mass transfer in fluids. This is due to the significant role of thermal radiation in the surface heat transfer

when convection heat transfer is small, particularly, in free convection problems involving absorbing-emitting fluids.

Nandeep et al. [1] analyzed MHD boundary layer flow past an exponentially permeable shrinking sheet of a Casson fluid. Hayat et al. [2] considered two-dimensional boundary layer flow of carreau fluid past a permeable stretching sheet. Raju, Sandeep [3] studied the effects of nonlinear thermal radiation and non-uniform heat source/sink in unsteady three-dimensional flow of Carreau and Casson fluids past a stretching surface in the presence of homogeneous heterogeneous reactions and the governing equations are solved by R-K based shooting method. Chakravarthula SK. Raju et al. [4] discussed the influence of thermal radiation and chemical reaction on the boundary layer flow of a MHD Jeffery Nano fluid over a permeable cone in the presence of thermophoresis Brownian motion effects. Casson fluid flow in the stagnation point region of a sphere with cross diffusion effects has been considered by Pushpalatha et al. [5]. Hakiem and Amin [6] have examined the influences of mass transfer on buoyancy induced flow over vertical flat plate embedded in a non-Newtonian fluid saturated porous medium. Najeeb Alam Khan and Faqiha Sultan [7] have considered the double diffusive Darcian convection flow of Eyring-Powell fluid from a cone embedded in a homogeneous porous medium with the effects of Soret and Dufour and the governing equations are numerically solved by non-perturbation scheme. Louis Gosselin, Alaxander K. da Silva [8] has been investigated to maximize the heat transfer rate removed from a warm plate by the Nano fluid. Chamkha and Aly [9] have obtained the numerical solution of steady natural convection boundary-layer flow of a nanofluid consisting of a pure fluid with nanoparticles along a permeable vertical plate in the presence of magnetic field, heat generation or absorption and suction or injection effects. The induced magnetic field effect on the stagnation point flow of a non-Newtonian fluid over a stretching sheet with homogeneous-heterogeneous reactions and non-uniform heat source or sink and the ordinary differential equations are numerically solved by R-K and Newton's method has been considered by Raju et al. [10]. The Magneto hydrodynamic three-dimensional boundary layer flow of an incompressible casson fluid in a porous medium has been obtained by Shehzad et al. [11]. Hayat et al. [12] have been investigated the mixed convection flow of non-Newtonian Nano fluid over a stretching surface in presence of thermal radiation, heat source/sink and first order chemical reaction. Raju et al. [13] have been analyzed the flow, heat and mass transfer behavior of casson fluid past an exponentially permeable stretching surface in presence of thermal radiation, magnetic field, viscous dissipation, heat source and chemical reaction. Nadeep et al. [14] have been studied magneto hydrodynamics Casson fluid flow in two lateral directions past a porous linear stretching sheet. Jasmine Benazir et al. [15] have been analyzed the effects of double dispersion, non-uniform heat source/sink and higher order chemical reaction on unsteady, free convective, MHD Casson fluid flow over a vertical cone and flat plate saturated with porous medium. Jagdish Prakash et al. [16] have been studied flow, heat and mass transfer characteristics of unsteady mixed convective magneto hydrodynamic flow of a heat absorbing fluid in an accelerated vertical wavy plate, subject to varying temperature and mass diffusion, with the influence of buoyancy, thermal radiation and Duffer effect. Shehzed et al. [17] have been investigated the convective heat and mass conditions in three-dimensional flow of an oldroyd-B Nano fluid and the governing problem solved numerically by convergent approximate solutions. The mixed convection boundary layer flow of a magneto hydrodynamic second grade fluid over an unsteady permeable stretching sheet discussed by Hayat and Qusim [18]. Parha et al. [19] have been analyzed the mixed convection flow and heat transfer from an exponentially stretching vertical surface in a quiescent fluid. Sajid and Hayat [20] have been studied the effect of radiation on the boundary layer flow and heat transfer of a viscous fluid over an exponentially stretching sheet. Anur Ishak [21] has been studied the effect of radiation on magneto hydrodynamic boundary layer flow of a viscous fluid over an exponentially stretching sheet. Mustafa et al. [22] have been discussed the unsteady flow and heat transfer of a Casson fluid over a moving flat plate with a parallel free stream. Mohammad Mehdi Rashidi et al. [23] have been examined heat and mass transfer in a steady two-dimensional magneto hydrodynamic viscoelastic fluid flow over a stretching vertical surface by considering Soret and Dufour effects. The boundary layer flow and heat transfer characteristic of second order fluid and second grade fluid with variable thermal conductivity and variation over an exponentially stretching sheet in porous medium have been studied by Singh et al.[24]. Iskandar Waini et al. [25] studied the effect of aligned magnetic field towards the flow and heat transfer of the upper-convected Maxwell (UCM) fluid over a Stretching/Shrinking sheet. Ali and Sandeep [26] investigated the heat transfer behavior of electrically conducting MHD flow of a Casson nanofluid over a Cone, wedge and a plate and a Cattaneo-Christov heat flex model with variable source/sink and nonlinear radiation effects. Anantha Kumar et al. [27] analyzed the thermo diffusion and diffusion thermo effects on MHD Casson fluid over a linear/nonlinear Stretching sheet and the governing equation are solved numerically using Range-Kutta based Shooting technique. The influence of aligned magnetic field on an unsteady flow of a Casson fluid past a vertical permeable oscillating plate in presence of radiation, chemical reaction and heat generation/absorption analyzed by Ramana Reddy et al.[28]. Ananth et al. [29] analyzed the Stagnation-point flow of a Casson fluid toward a stretching sheet with nonlinear thermal radiation and induced magnetic field effects. The induced magnetic field and non-uniform heat Source or Sink effects on the stagnation-point flow of

a non-Newtonian fluid towards a stretching sheet in the presence of homogeneous-heterogeneous reaction investigated by Raju et al. [30]. Naveed Ahmed et al. [31] discussed squeezing flow of an electrically conducting Casson fluid has been taken into accound and the governing equations are solved analytically by using the variation of parameters method.

Thus the present's investigation is concerned with the study of variable magnetic field effect and radiative Casson fluid in two dimensional MHD flow, heat and mass transfer of viscous incompressible fluid pass a permeable vertical plate in a porous medium. The effects of various physical parameters on the velocity, temperature and concentration profiles as well as on local skin friction co-efficient and local Nusselt number are shown graphically.

2.Formulation of the Problem

Consider two dimensional laminar boundary layer flow of a viscous incompressible electrically conducting and heat absorbing fluid fast a semi-infinite vertical permeable plate embedded in a uniform porous medium which is subject to thermal and concentration buoyancy effects. As shown in Fig.1, $\hat{x}$ - axis is along the plate and $\hat{y}$ - is perpendicular to the plate. The wall maintained at a constant temperature T_w and concentration C_w higher than the ambient temperature T_∞ and concentration C_∞ respectively. Also, it is assumed that there exists a homogeneous chemical reaction of first order with rate constant R between the diffusing species and the fluid.

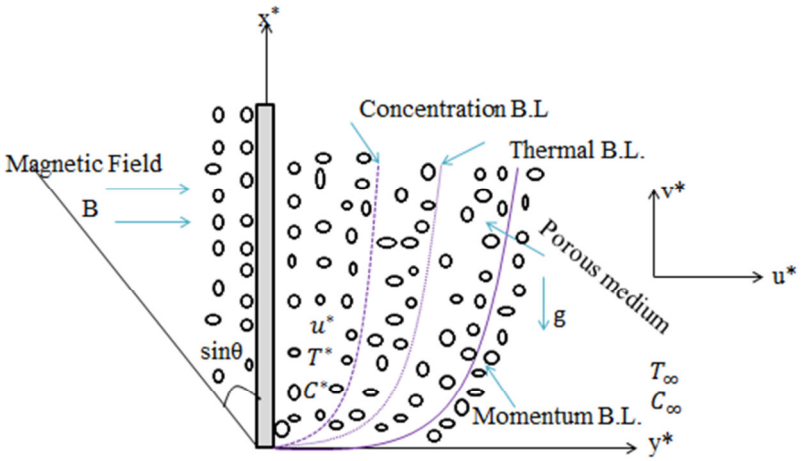

Fig.1. Physical configuration of problem.

The physical situation which can be written as

$$\frac{d\hat{v}}{d\hat{y}} = 0 \tag{1}$$

i.e., $\hat{v} = -v_0$ (Constant) (2)

$$\frac{d\hat{p}}{d\hat{y}} = 0 \Rightarrow \hat{p} \quad \text{is independent of} \quad \hat{y} \tag{3}$$

$$\rho\left(\hat{u}\frac{d\hat{u}}{d\hat{x}} + \hat{v}\frac{d\hat{u}}{d\hat{y}}\right) = \mu\left(1+\frac{1}{\beta}\right)\frac{d^2u}{dy^2} - \sigma B_0^2 \sin^2\delta u + \rho g\beta_T\left(\hat{T}-T_\infty\right) + \rho g\beta_c\left(\hat{C}-C_\infty\right) \tag{4}$$

$$\rho c_p\left(\hat{u}\frac{d\hat{T}}{d\hat{x}} + \hat{v}\frac{d\hat{T}}{d\hat{y}}\right) = \alpha\frac{d^2T}{dy^2} + \mu\left(1+\frac{1}{\beta}\right)\left(\frac{d\hat{u}}{d\hat{y}}\right)^2 - \frac{\partial\hat{q}_r}{\partial y} + \sigma B_0^2 u^2 \tag{5}$$

$$\hat{v}\frac{d\hat{C}}{d\hat{y}} = D\frac{d^2C}{dy^2} - R\left(\hat{C}-C_\infty\right) \tag{6}$$

Where $\hat{u}$ and $\hat{v}$ are the components of dimensional velocity along $\hat{x}$ and $\hat{y}$ directions respectively. α is the fluid thermal diffusivity. The fourth and fifth terms on RHS of the momentum equation (4) denote the thermal and concentration buoyancy effects respectively. Also second and fourth terms of the RHS of energy equation (5)

represents the viscous dissipation and ohmic dissipation respectively. The third and fifth term on the RHS of Eq. (5) denote the inclusion of the effect of thermal radiation and heat absorption effects respectively.
The radiative heat flux is given by

$$\frac{\partial \hat{q}_r}{\partial \hat{y}} = 4\left(\hat{T} - T_\infty\right) I' \tag{7}$$

Where $I' = \int_0^\infty K_{\lambda w} \frac{\partial \rho_{b\lambda}}{\partial \hat{T}} d\lambda$, $K_{\lambda w}$ is the absorption coefficient at the wall and $e_{b\lambda}$ is Planck's function.

The appropriate boundary conditions for velocity, temperature and concentration fields are

$$\hat{y} = 0 : u = 0,\ \hat{T} = T_w,\ \hat{C} = C_w \tag{8}$$

$$\hat{y} \to \infty : u \to 0,\ \hat{T} \to T_\infty,\ \hat{C} \to C_\infty \tag{9}$$

where C_w and T_w are the wall dimensional concentration and temperature respectively.
Introducing the following non-dimensional quantities:

$$\left.\begin{aligned} y = \frac{v_0 \hat{y}}{v},\ u = \frac{\hat{u}}{v_0},\ M^2 = \frac{B_0^2 v^2 \sigma}{v_0^2 \mu},\\ K = \frac{\hat{K} v_0^2}{v^2},\ \theta = \frac{\hat{T} - T_\infty}{T_w - T_\infty},\ C = \frac{\hat{C} - C_\infty}{C_w - C_\infty}, \end{aligned}\right\} \tag{10}$$

Using (7) and (10) in Eqs. (4) - (6), we get the following non-dimensional equations:

$$\left(1 + \frac{1}{\beta}\right)\frac{d^2 u}{dy^2} + \frac{du}{dy} - M^2 \sin^2 \delta u = -Gr\theta - GmC \tag{11}$$

$$\frac{d^2\theta}{dy^2} + \Pr\left(\frac{d\theta}{dy}\right) + E\Pr\left(1 + \frac{1}{\beta}\right)\left(\frac{du}{dy}\right)^2 - \Pr F\theta + \Pr EM^2 u^2 = 0 \tag{12}$$

$$\frac{d^2 C}{dy^2} + Sc\frac{dC}{dy} - Sc\gamma C = 0 \tag{13}$$

where Gr is the Grashof number, Gm is the solutal Grashof number, $\Pr$ is the Prandtl number, M is the magnetic field parameter, F is the radiation parameter, Sc is the Schmit number, E is the Eckert number, ϕ is the heat source parameter and γ is the chemical reaction parameter and K is the permeability defined as follows:

$$\left.\begin{aligned} E = v_0^2 / C_p\left(T_w - T_\infty\right),\ \Pr = \mu C_p / \alpha,\ Gr = \rho g \beta_T v^2 \left(T_w - T_\infty\right) / v_0^3 \mu\\ Sc = v \Big/ D,\ \ Gm = \frac{\rho g \beta_c \left(C_w - C_\infty\right)}{v_0^3}\frac{v^2}{\mu},\ \ F = \frac{4vI'}{\rho C_p v_0^2},\\ \gamma = \frac{Rv}{v_0^2},\ \phi = \frac{Q_0 v}{\rho C_p v_0^2}, \end{aligned}\right\} \tag{14}$$

The corresponding boundary conditions in dimensionless form are

$$y = 0 : u = 0,\ \theta = 1,\ C = 1 \tag{15}$$

$$y \to \infty : u \to 0,\ \theta \to 0,\ C \to 0 \tag{16}$$

3.Method of Solution

Eqs. (11) – (13) represent a set of partial differential equations that cannot be solved in closed form. However, these equations can be solved analytically after reducing them to a set of ordinary differential equations in dimensionless form. Thus we can represent the velocity u , temperature θ , and concentration C in terms of power of Eckert number E as in the flow of an incompressible fluid Eckert number is always less than unity since the flow due to the joules dissipation is super imposed on the main flow. Hence, we can assume

$$\left.\begin{aligned} u(y) &= u_0(y) + Eu_1(y) + o(E^2) \\ \theta(y) &= \theta_0(y) + E\theta_1(y) + o(E^2) \\ C(y) &= C_0(y) + EC_1(y) + o(E^2) \end{aligned}\right\} \tag{17}$$

Substituting (17) in Eqs. (11) – (13) and equating the coefficient of zeroth powers of $E\left(i.e.O\left(E^0\right)\right)$, we get the following set of equations:

$$\left(1+\frac{1}{\beta}\right)u_0'' + u_0' - P_1 u_0 = -Gr\theta_0 - GmC_0 \tag{18}$$

$$\theta_0'' + \Pr\theta_0' - \Pr F\theta_0 = 0 \tag{19}$$

$$C_0'' + ScC_0' - Sc\gamma C_0 = 0 \tag{20}$$

Next equating the coefficients of first-order of $E\left(i.e.O\left(E^1\right)\right)$, we obtain

$$\left(1+\frac{1}{\beta}\right)u_1'' + u_1' - P_1 u_1 = -Gr\theta_1 - GmC_1 \tag{21}$$

$$\theta_1'' + \Pr\theta_1' + \Pr\left(1+\frac{1}{\beta}\right)u_0'^2 - \Pr F\theta_1 + \Pr P_2 u_0^2 = 0 \tag{22}$$

$$C_1'' + ScC_1' - Sc\gamma C_1 = 0 \tag{23}$$

where $P_1 = M^2\sin^2\delta$ and $P_2 = M^2$ the corresponding boundary conditions are

$$y = 0 : u_0 = 0,\ u_1 = 0,\ \theta_0 = 1,\ \theta_1 = 0,\ C_0 = 1,\ C_1 = 0 \tag{24}$$

$$y \to \infty : u_0 \to 0,\ u_1 \to 0,\ \theta_0 \to 0,\ \theta_1 \to 0,\ C_0 \to 0,\ C_1 \to 0. \tag{25}$$

We have restricted the solution of velocity, temperature and concentration fields up to $O(E)$ and neglected the higher order of $O\left(E^2\right)$ as the value of $E << 1$. Without going into the details, solutions of Eqs. (18) – (23) with the help of boundary conditions, (24) and (25) are obtained the follows:

$$u_0 = A_3\left(e^{-A_2 y} - e^{-A_1 y}\right) + A_4\left(e^{-A_2 y} - e^{-m_1 y}\right) \tag{26}$$

$$\theta_0 = e^{-A_1 y} \tag{27}$$

$$C_0 = e^{-m_1 y} \tag{28}$$

$$u_1 = B_{17}e^{-A_2 y} - B_{10}e^{-A_1 y} + B_{11}e^{-2A_1 y} + B_{12}e^{-2A_2 y} - B_{13}e^{-A_5 y} + B_{14}e^{-2m_1 y} - B_{15}e^{-B_1 y} + B_{16}e^{-B_2 y} \tag{29}$$

$$\theta_1 = B_9 e^{-A_1 y} - B_3 e^{-2A_1 y} - B_4 e^{-2A_2 y} + B_5 e^{-A_5 y} - B_6 e^{-2m_1 y} + B_7 e^{-B_1 y} - B_8 e^{-B_2 y} \tag{30}$$

$$C_1 = 0 \tag{31}$$

The physical quantities of interest are the wall shear stress τ_w is given by

$$\tau_w = \mu\left.\frac{\partial\hat{u}}{\partial\hat{y}}\right|_{\hat{y}=0} = \rho v_0^2 u'$$

Therefore, the local skin friction C_{f_x} is given by

$$C_{f_x} = \frac{\tau_w}{\rho v_0^2} = u'(0) \tag{32}$$

Using (17), (26) and (29) in (32), we get

$$\begin{aligned} C_{f_x} &= A_3\left(A_1 - A_2\right) + A_4\left(m_1 - A_2\right) \\ &\quad - E\left[B_{17}A_2 - B_{10}A_1 + 2B_{11}A_1 + 2B_{12}A_2 - B_{13}A_5 + 2B_{14}m_1 - B_{15}B_1 + B_{16}B_2\right] \end{aligned} \tag{33}$$

The local surface heat flux is given by

$$q_w = -k\left.\frac{\partial \hat{T}}{\partial \hat{y}}\right|_{\hat{y}=0}$$

where k is the effective thermal conductivity. The local Nusselt number $Nu_x = q_w/\left(T_w - T_\infty\right)$ can be written as

$$\frac{Nu_x}{\mathrm{Re}_x} = \theta'(0) = -\left.\frac{\partial \theta}{\partial y}\right|_{y=0} \tag{34}$$

Using (17), (27) and (30) in (34), we get

$$\frac{Nu_x}{\mathrm{Re}_x} = A_1 + E\left[B_9 A_1 - 2B_3 A_1 - 2B_4 A_2 + B_5 A_5 - 2B_6 m_1 + B_7 B_1 - B_2 B_8\right] \tag{35}$$

The local surface mass flux is given by

$$\frac{Sh_x}{\mathrm{Re}_x} = \left.\frac{\partial C}{\partial y}\right|_{y=0} \tag{36}$$

Using (11), (22) and (25) in (30), we get

$$\frac{Sh_x}{\mathrm{Re}_x} = -m_1 \tag{37}$$

where $\mathrm{Re}_x = v_0 k / v$ is the local Reynolds number.

4.Results and Discussion

In this work we have obtained analytical solutions of velocity field, temperature and concentration field in the study of mixed convection flow of a viscous incompressible electrically conducting fluid over an infinite vertical porous plate in the presence of magnetic field and radiative casson fluid flow computed results are presented in graphical form. We have extracted interesting insights regarding the influence of all the physical parameters that govern the problem. The influence of $\mathrm{Pr} = 7.0$, $Gm = 2.0$, $F = 3.0$, $M = 2.0$, $Gr = 4.0$, $Sc = 2.0$, $\theta = 0.6, \gamma = 0.1, \beta = 0.5, \phi = 2.0, E = 0.01$ on the velocity, temperature and concentration profile can be analyzed from fig. 2-12 and on skin friction coefficient and Nusselt number in fig. 13-19.

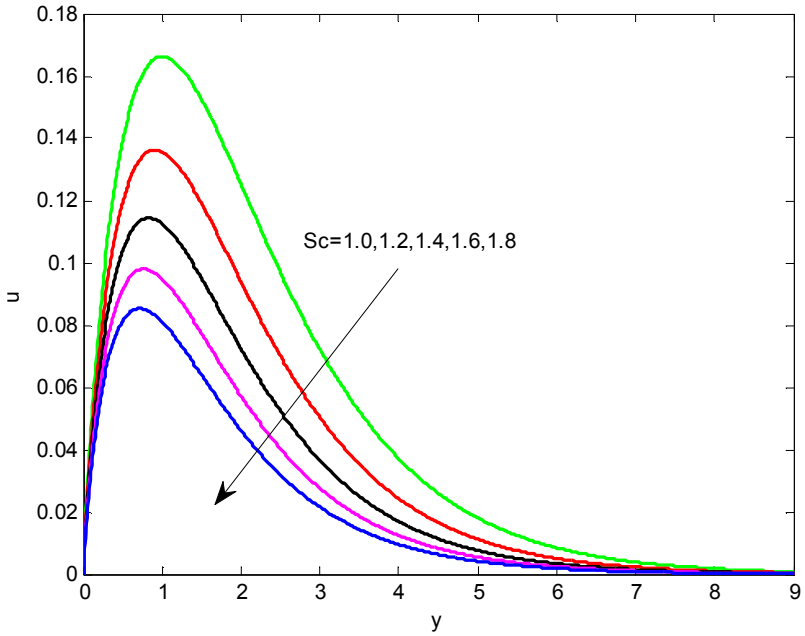

Fig.2. Velocity profiles for different values of Scmidt number.

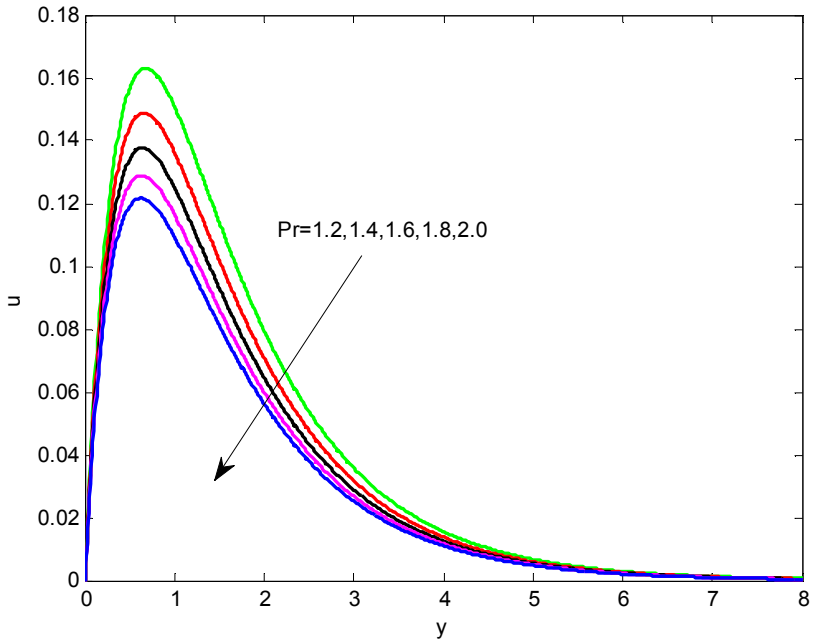

Fig.3. Velocity profiles for different values of Prandtl number.

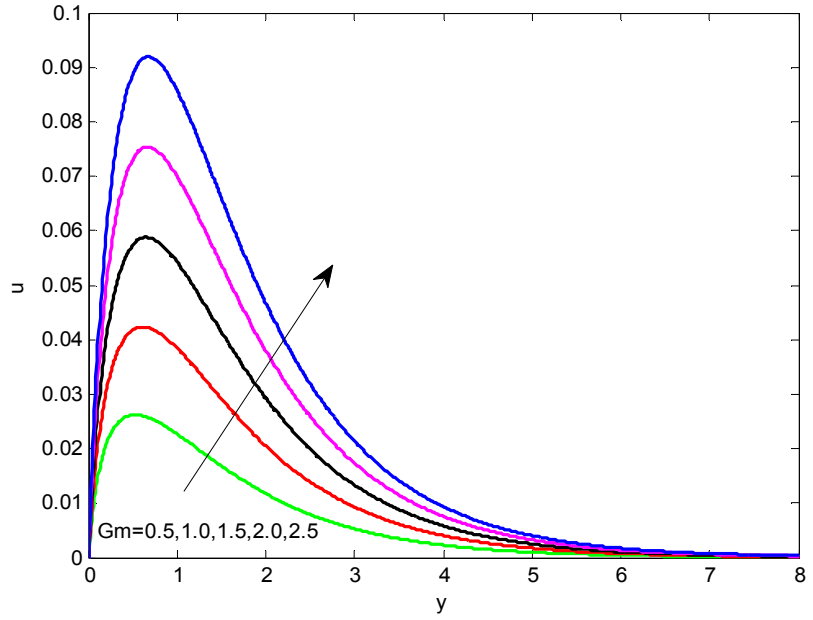

Fig.4. Velocity profiles for different values of solutal Grashof number.

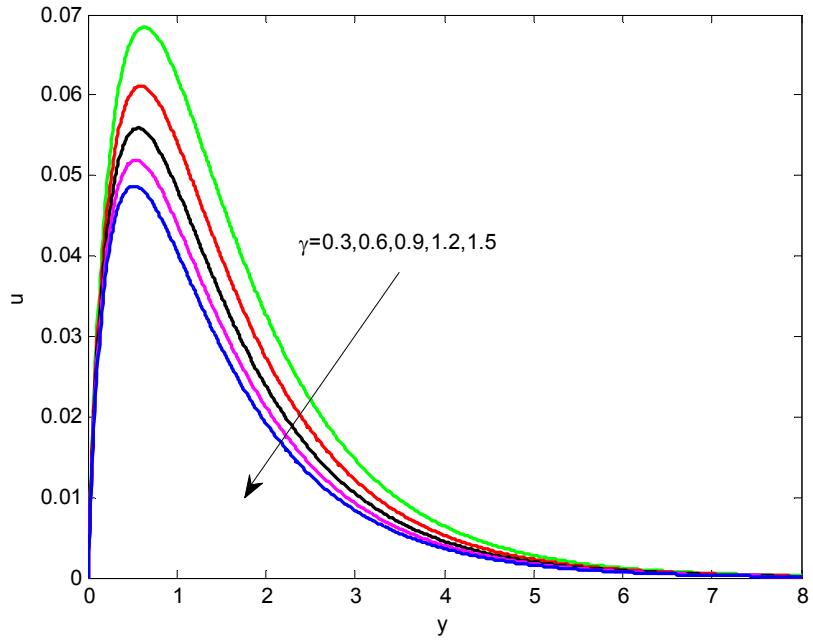

Fig.5. Velocity profiles for different values of chemical reaction parameter.

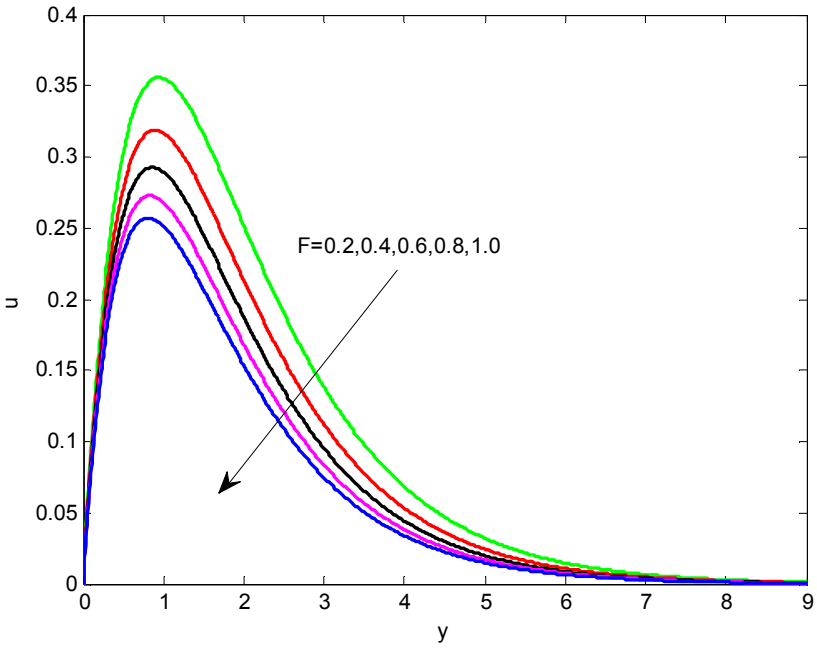

Fig.6. Velocity profiles for different values of radiation parameter.

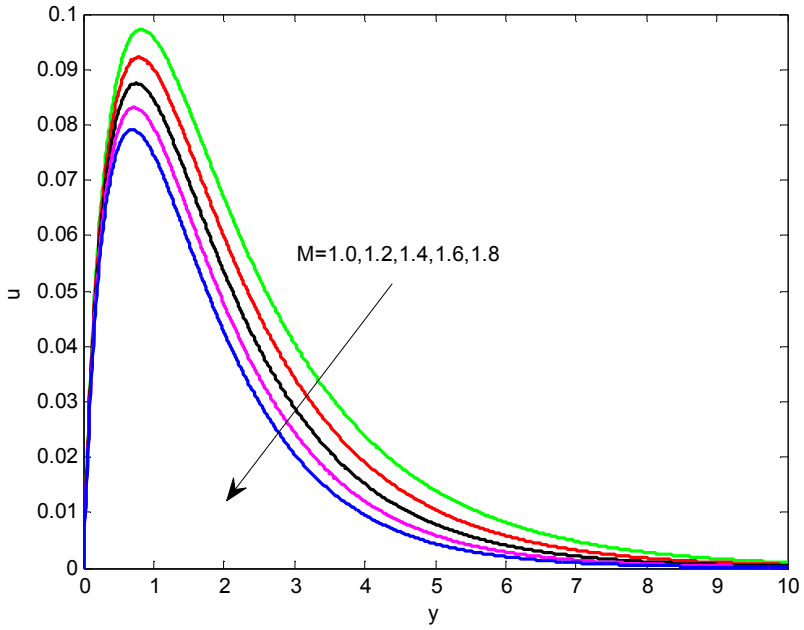

Fig.7. Velocity profiles for different values of magnetic field parameter.

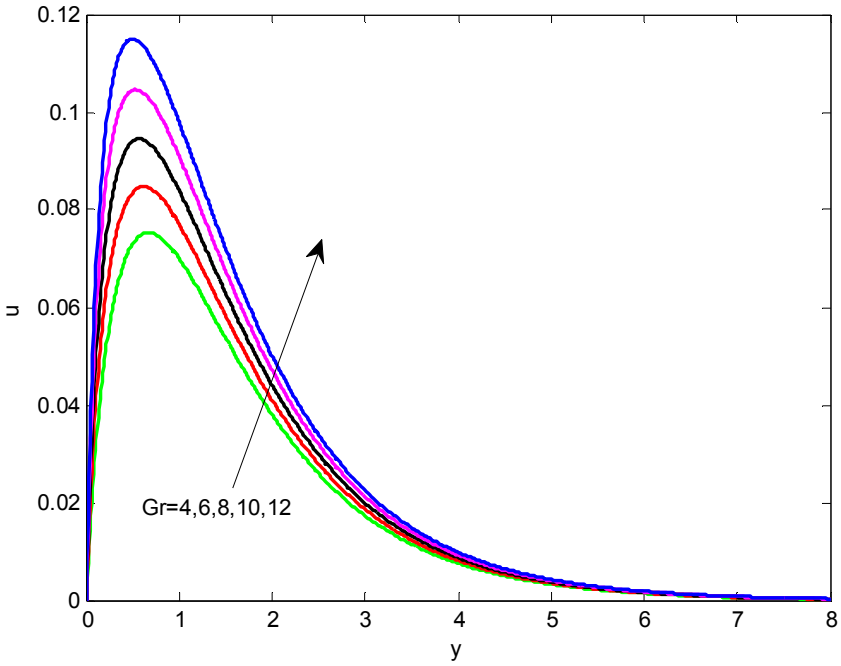

Fig.8. Velocity profiles for different values of Grashof number.

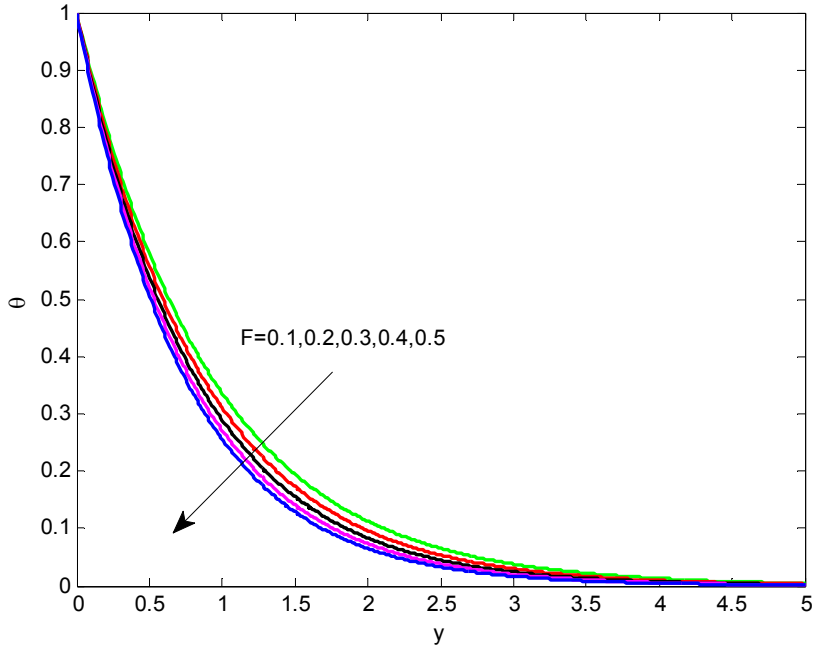

Fig.9. Temperature profiles for different values of radiation parameter.

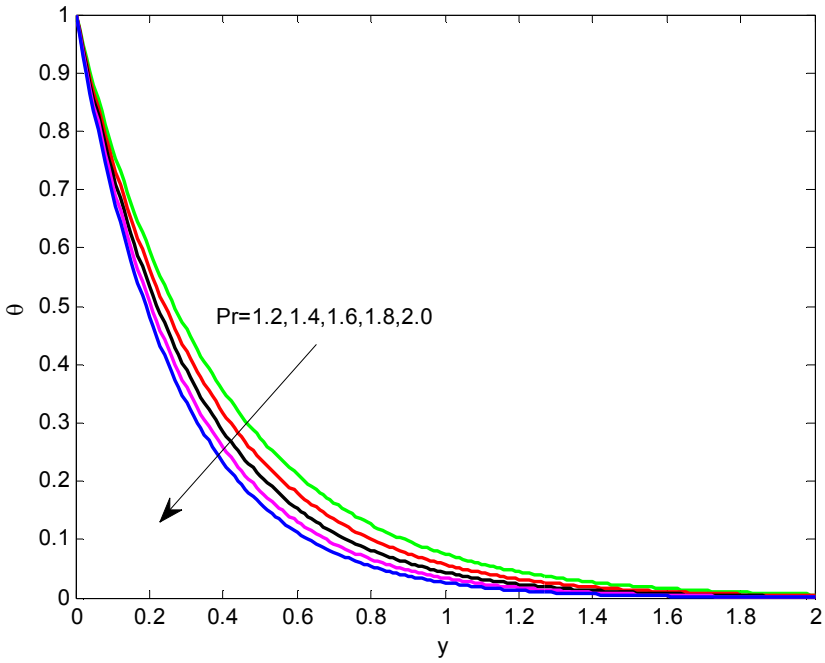

Fig.10. Temperature profiles for different values of Prandtl number.

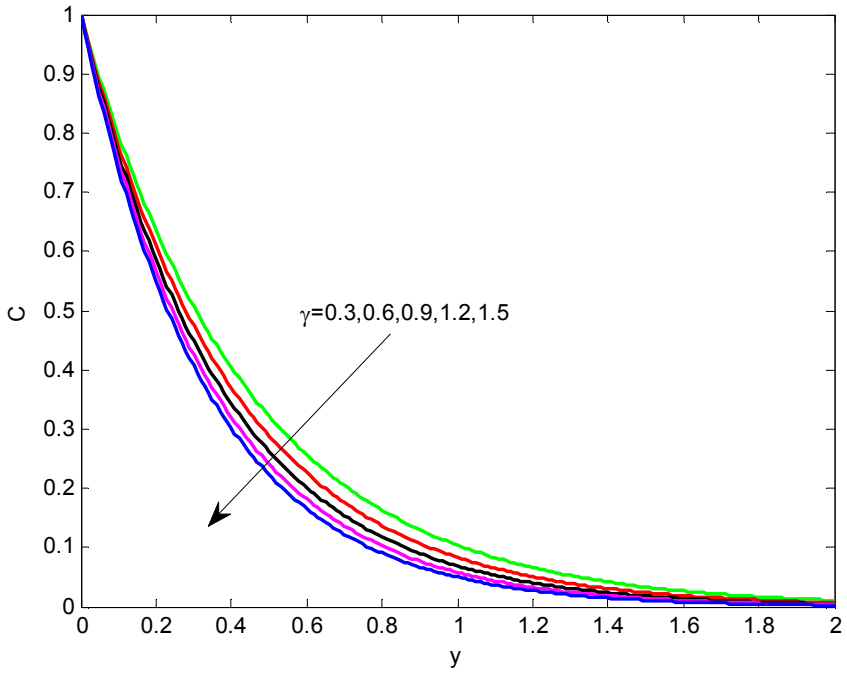

Fig.11. Concentration profiles for different values of chemical reaction parameter.

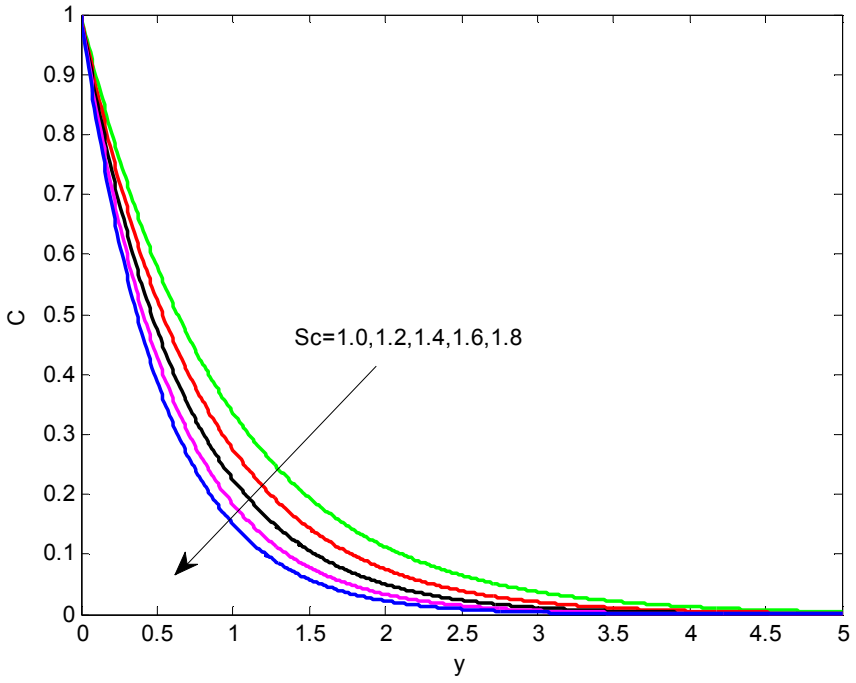

Fig.12. Concentration profiles for different values of Schmit number .

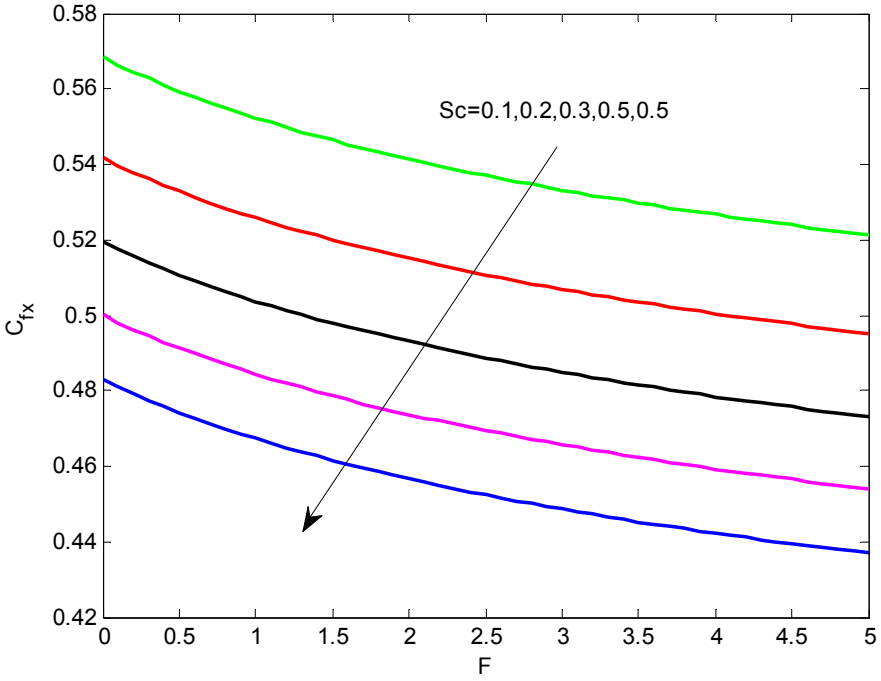

Fig.13. Variation of skin-friction coefficient for different values of Sc with F .

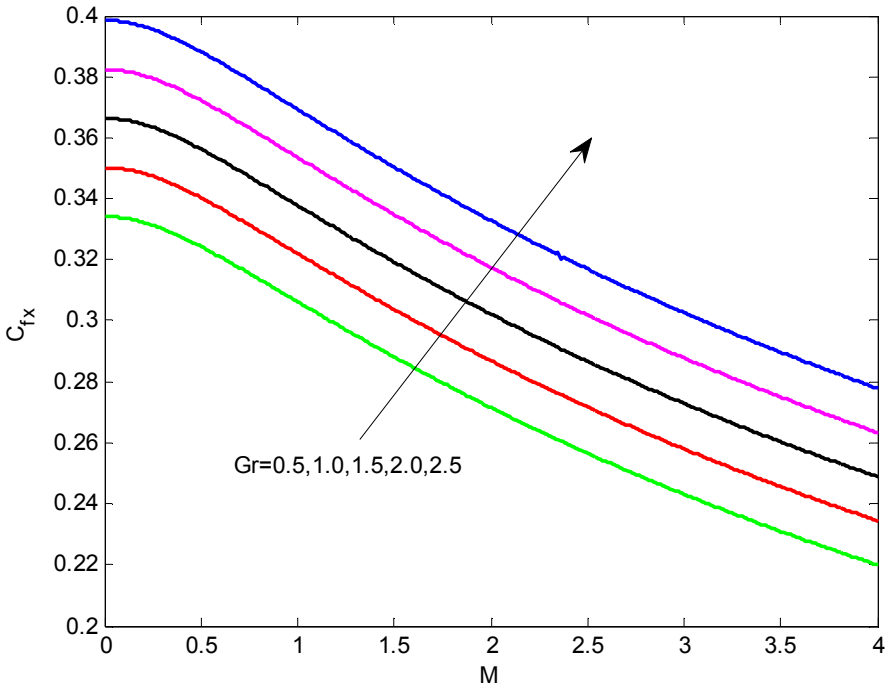

Fig.14. Variation of skin-friction coefficient for different values of Gr with M .

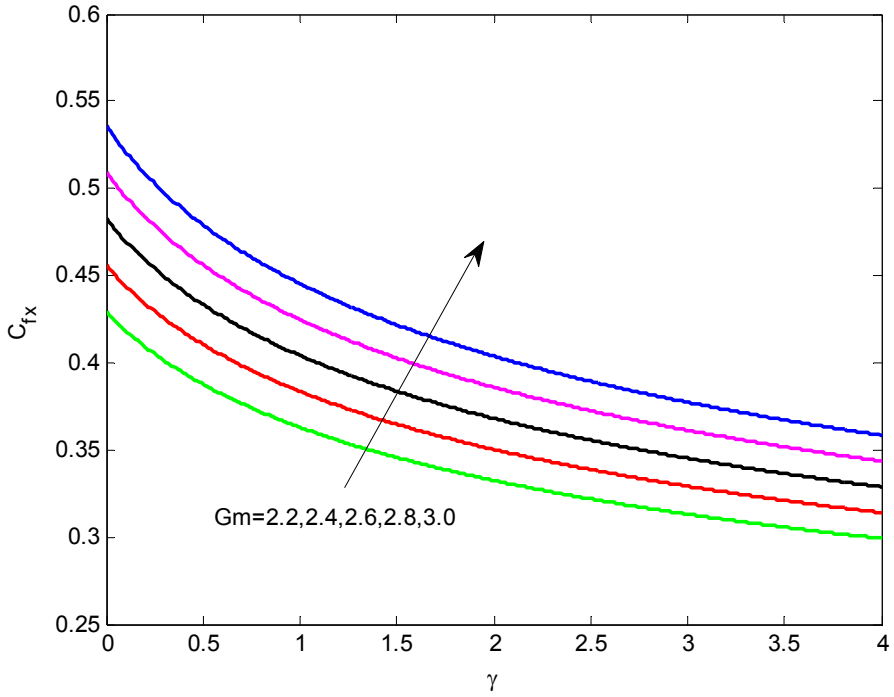

Fig.15. Variation of skin-friction coefficient for different values of Gm with γ

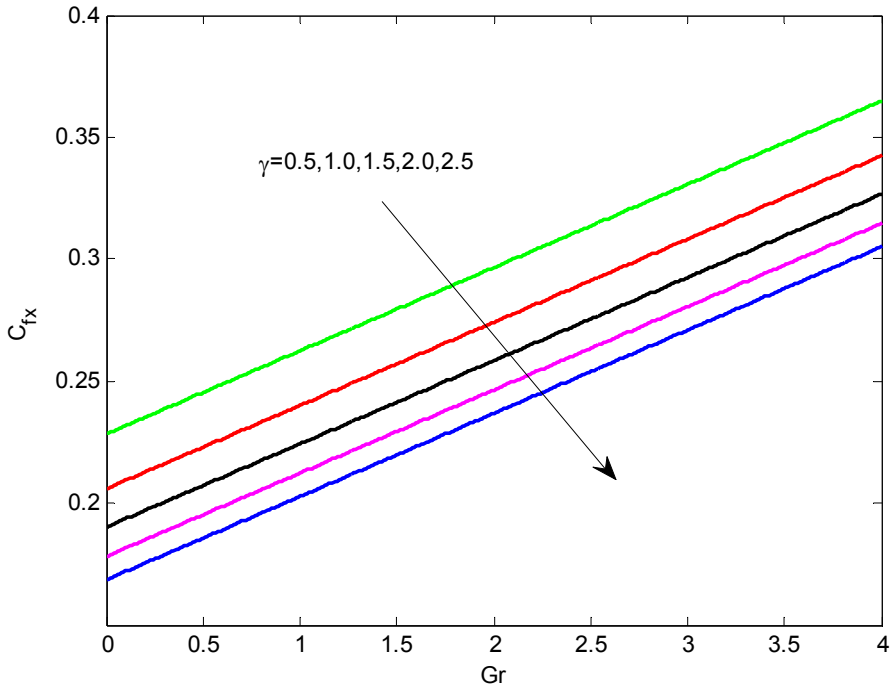

Fig.16. Variation of skin-friction coefficient for different values of γ with Gr.

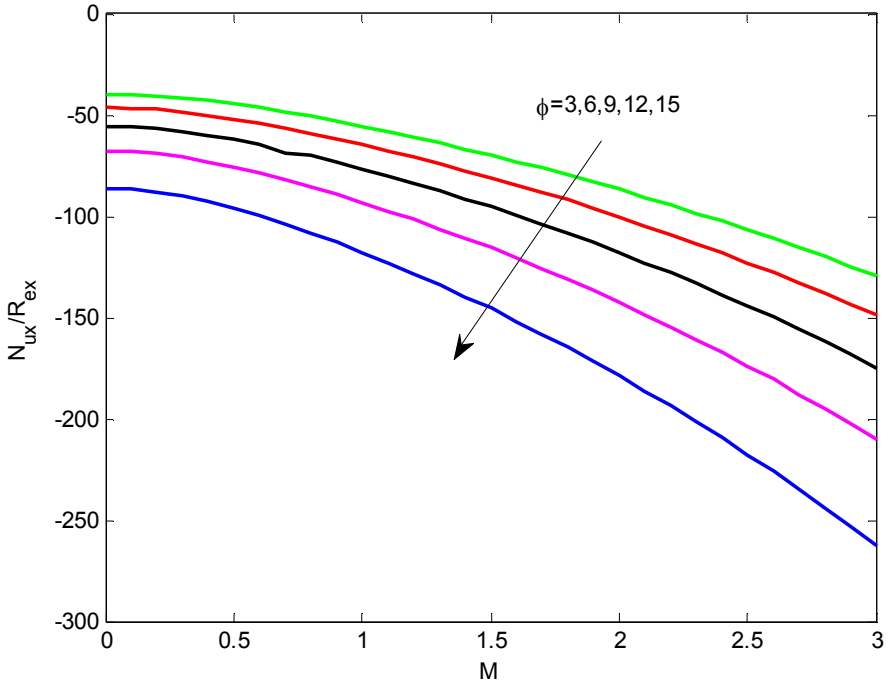

Fig.17. Variation of Nusselt number for different values of ϕ with M .

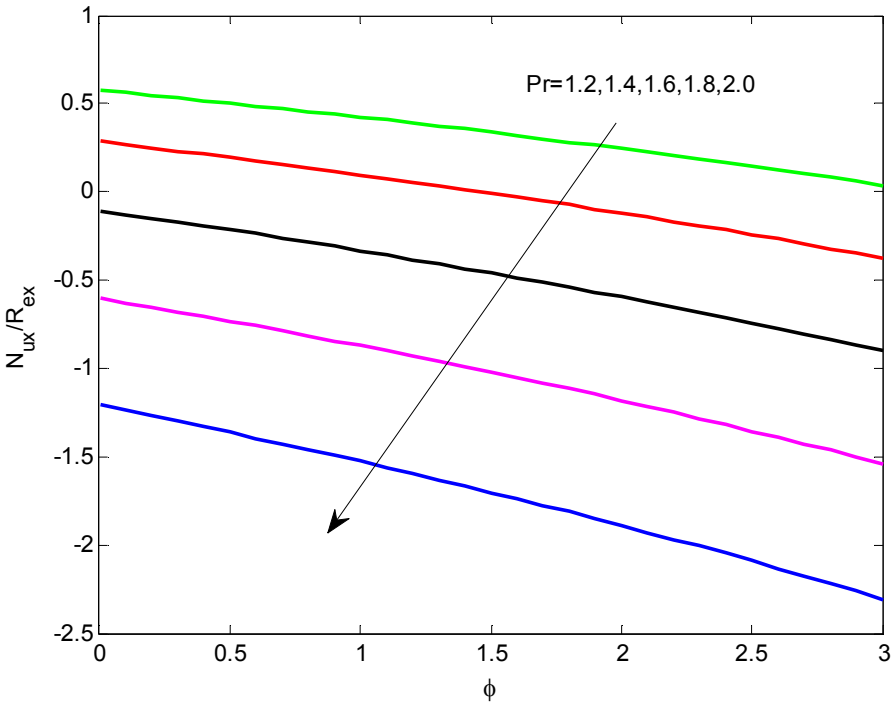

Fig.18. Variation of Nusset number for different values of $\Pr$ with ϕ .

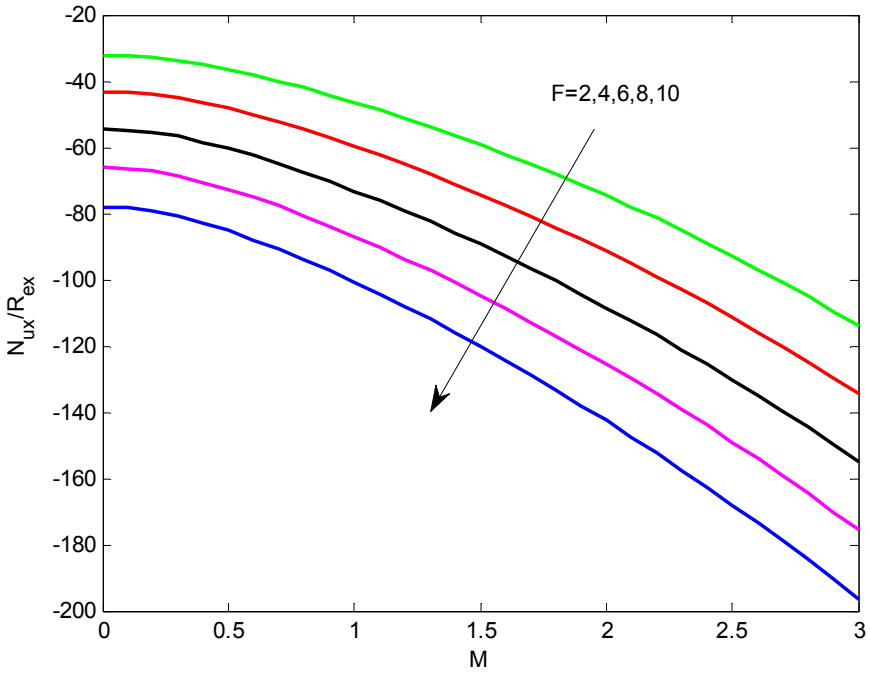

Fig.19. Variation of Nusselt number for different values of F with M .

We observe from Fig.2 given that value of schmit number ($Sc = 1.0$) increase in the peak velocity is seen near the plate. Whereas for higher values of schmit number ($Sc = 1.8$) the peak velocity shifts closer to the plate. Further, it is observed that the concentration boundary layer decreases with increasing values in Sc . Fig.3 depicts the effect of radiation on the horizontal velocity. We note from this figure that there is decrease in the value of horizontal velocity with increase in the Prandtl number $\Pr$. Which shows the fact that increase in Prandtl number decrease the velocity in the boundary layer due to decrease in the boundary layer thickness.

Fig.4 shows that increase in the solutal Grashof number increases velocity in the momentum boundary layer. It is further noted that the peak value of velocity increases rapidly near the surface as the value of Gm decrease. The effect of chemical reaction parameter γ is highlighted in Fig.5.which shows that the velocity decreases with increasing the rate of chemical reaction parameter γ . Hence increase the chemical reaction rate parameter leads to a fall in the momentum boundary layer.

We note from Fig.6 that there is decrease in the value of horizontal velocity with increase in radiation parameter F. which shows the fact that increase in radiation parameter decrease the velocity in the boundary layer due to decrease in the boundary layer thickness. Fig.7 from the effect of magnetic field parameter M shown that the velocity decreases with increasing the rate of magnetic field parameter M . Hence increase the magnetic field parameter lead to decrease in the horizontal boundary layer. The variation of velocity profile against y is depicted in Fig.8 for various values of Gr . It is observed that an increasing in Gr leads to an increasing in the velocity field. In addition, the curves show that the peak value of velocity increases rapidly near the surface as the value of Gr increases.

The increase of the radiation parameter F leads decrease the boundary layer thickness and thereby decrease in the value of the heat transfer in the presence of thermal and solutal buoyancy force as shown in Fig.9.similarly the effect is seen by increasing the value of prandtl number as depicted in Fig.10. This is due to the fact that the thermal boundary layer absorbs energy which causes the temperature fall considerably with increasing the value of prandtl number $\Pr$.

The effect of the reaction rate parameter γ on the species concentration profiles for generative chemical reaction is shown in Fig.11. It is noticed from the graph that there is marked effect with increasing the value of the chemical reaction rate parameter γ on concentration distribution in the boundary layer. It is clearly observed from this figure that the concentration of species value of $\gamma = 1.5$ at vertical plate decrease till it attains the minimum value of zero at the end of the boundary layer and this trend is seen for all the values of reaction rate parameter. Further, it is observed that increasing the value of the chemical reaction decreases the concentration

of species in the boundary layer; this is due to the fact that boundary layer decreases with increasing in the value of γ. Similarly facts are seen in the case when Schmidt number is increased as noted in Fig.12. It may also be observed from this figure that the effect of Schmidt number Sc on concentration distribution decreases slowly for higher values of Sc. As can be expected that the mass transfer rate increases as γ increasing with all other parameter fixed. ie. An increase in the Schmidt number Sc produces decrease in the concentration boundary layer thickness associated with the reduction in the concentration profiles. Physically, the increase in the value of Sc means decrease of molecular diffusion D. Hence the concentration of the species is higher for smaller values of Sc and lower for larger values of Sc.

Figs.13-19 presents the variation of the local skin friction coefficient C_{f_x} and the local Nusselt number Nu_x / Re_x with various values of Sc, Gr, Gm, γ, ϕ, Pr, F and M. Fig.13 shows that increasing the value of Schmidt number with F to seen that skin friction is higher for heavier particle $Sc = 0.5$ than lighter particle $Sc = 0.1$.

Figs.14-16 represents the skin friction coefficient for different values Gr, Gm and γ to corresponded parameters M, γ and Gr respectively. It is found that Grashof, solutal Grashof rates increase the effects of increasing the skin friction coefficient. But Chemical reaction rates increase the effects of decreasing the skin friction coefficient.

Figs.17-19 displays the heat transfer coefficient in terms of parameters M, ϕ and M corresponding to the different values of ϕ, Pr and F. This figure clearly shows that the Nusselt number decreases with increasing the value of magnetic field parameter, whereas increasing the value of ϕ, Pr and F decreases the value of the Nusselt number.

5. Conclusions

- In this study, we have to investigate the influence of thermal radiation and magnetic field with Casson fluid flow past a vertical plate. The nonlinear and governing equations are solved analytically by perturbation technique.
- Velocity, Temperature and Concentration profiles as well as local skin friction coefficient and local Nusselt number are presented graphically and analyzed.
- It is found that the Velocity, Temperature and Concentration decreases with increasing the values of Sc, Pr, γ, F, M and the reverse trend is seen by increasing the value of Gr and Gm.
- Also concluded that the Grashof number and solutal Grashof number is to increase skin friction coefficient with magnetic field and chemical reaction increasing the skin friction coefficient.
- Finally the presence of heat source and thermal radiation decreases the value of Nusselt number with increasing the values of ϕ and Pr and F with corresponding parameters M, ϕ and M.

References

Ali,M.E. & Sandeep,N. (2017), "Cattaneo-Chritov model for radiative heat transfer of magneto hydrodynamic Casson-ferrofluid : A numerical study", Results in physics, 721-30.

Ananth, Dinesh,P.A., Sugunamma,V. & Sandeep, N. (2015), "Effect of Nonlinear Thermal Radiation On Stagnation Flow of a Casson Fluid towards a Stretching Sheet", IISTE, 5(8).

Anantha Kumar,K.., Ramana Reddy,J.V., Sandeep,N. & Sugunamma,V. (2016), "Dual Solution for Thermo Duffusion and Duffusion Effects on 3D MHD Casson Fluid Flow over a Stretching Surface", Research J.Pharm and Tech.9 (8).

Anur Ishak. (2011), "MHD Boundary Layer Flow Due to an Exponentially Stretching sheet with Radiation Effect", Sains Malaysiana 40(4), 391-395.

Chakravarthula SK Raju., Macharla Jayachandra Babu. & Naramgari Sandeep. (2016), "Chemically reacting radiative MHD Jeffery nanofluid flow over a cone in porous medium", International Journal of Engineering Research in Africa Vol.19 pp 75-90.

Chamkha,A.J. & Aly,A.M.(2011), "MHD Free Convection Flow of a Nanofluid past a vertical plate in the presences of Heat Generation or Absorption Effects", Chem.Eng.Comm., 198, 425-441.

Hakiem,M.A.EI. & Amin,M.F.EI. (2001), "Mass transfer effects on the non-Newtonian fluid past a vertical plate embedded in a porous medium with non-uniform surface heat flux", Heat and Mass Transfer, 37293-297.

Hayat,T. & Qasim,M. (2011), "Radiation and magnetic field effects on the unsteady mixed convection flow of a second grade fluid over a vertical stretching sheet", Int.J.Numer. Meth.Fluid, 66, 820-832.

Hayat,T., Sadia Asad., Mustafa,M. & Alsaedi,A. (2014), "Boundary layer flow of carreau fluid over a convectively heated stretching sheet", Applied Mathematics and Computation 246, 12-22.

Hayat,T., Bilal Ashraf,M., Shehzad,S.A. & Alsaedi, A. (2015), "Mixed convection Flow of Casson Nanofluid over a Stretching Sheet with Convectively Heated Chemical Reaction and Heat Source/Sink", Journal of Applied Fluid Mechanics, 8(4), 803-813.

Iskandar Waini., Nurul Amira Zainal. & Najiyah Safwa Khashi. (2017), "Aligned Magnetic Field Effects on Flow and Heat Transfer of theUpper-Convected Maxwell Fluid over a Stretching/Shrinking Sheet", MATEC Web Conference 97, 01073.

Jagdish Prakash., Bangalore Rushi Kumar & Ramachandra Sivaraj. (2014), "Radiation and Dufour Effects on Unsteady MHD Mixed Convective Flow in an Accelerated Vertical Wavy Plate with Varying Temperature and Mass Diffussion", Walailak J Sci and Tech 11(11), 939-954.

Jasmine Benazir, A., Sivaraj,R. & Makinde,O.D. (2016) , "Unsteady Magnetohydrodynamic Casson fluid flow over a vertical cone and flat plate with non-uniform heat source/sink", International Journal of Engineering Research in Africa 2, 69-83.

Louis Gosselin. & Alexander K. da Silva. (2004) , combined "Heat transfer and power dissipation" optimization of nanofluid flow, Applied physics letters 85, 18.

Mohammad Mehdi Rashidi., Mohamed Ali., Behnam Rostami., Peyman Rostami. & Gong- Nan Xie. (2015), "Heat and Mass Transfer for MHD Viscoelastic Fluid Flow over a Vertical Stretching Sheet with Considering Soret and Dufour Effects", Hindawi publishing Corporation Mathematical problem in Engineering 12.

Mustafa,M., Hayat,T., Pop,I. & Aziz,A. (2011), "Unsteady Boundary Layer Flow of a Casson Fluid Due to an Impulsively Started Moving Flat Plate", Heat Transfer-Asian Research, 40(6).

Nadeep,S., Rizwan UI Haq. & Lee,C. (2012), "MHD flow of casson fluid over an exponentially shrinking sheet", Scientia Iranica B 19(6), 1550-1553.

Nadeep,S., Rizwan UI Haq., Noreen Sher Akbar. & Khan,Z.H. (2013) , "MHD three-dimensional casson fluid flow past a porous linearly stretching sheet", Alexandria Engineering Journal 52, 577-582.

Najeeb Alam Khan. & Faqiha Sultan. (2015), "On the double diffusive Convection flow of Eyring- Powell fluid due to cone through a porous medium with Soret and Dufour effects", AIP Advances 5, 057140.

Naveed Ahmed., Umar Khan., Sheikh Irfanullah Khan., Saima Bano. & Syed Tauseef Mohyud-Din. (2015), "Effects on magnetic field in squeezing flow of a Casson fluid between Parallel Plates", Journal of King Saud University Science.

Partha, M.K., Murthy, PVSN. & Rajasekhar, GP. (2005), ''Effect of viscous dissipation on the mixed convection heat transfer from an exponentially stretching surface", Heat Mass Transfer 41, 360-366.

Pushpalatha,K., Sugunamma,V., Ramana Reddy,J.V. & Sandeep N. (2016), "Dufour and Soret Effects on Unsteady Flow of a Casson Fluid in the Stagnation Point Region of a Rotating Sphere", Middle-East Journal of Scientific Research 24 (4),1141-1150.

Raju,C.S.K., Sandeep,N. & Saleem,S. (2015), "Homogeneous-hetrogeneous reactions on stagnation-point flow of a Casson fluid with induced magnetic field".

Raju,C.S.K.., & Sandeep,N. (2016) "Unsteady three-dimensional flow of Casson-Carreau fluids past a stretching surface", Alexandria Engineering Journal 55, 1115-1126.

Raju,C.S.K., Sandeep,N. & Saleem,S. (2016) , "Effects of induced magnetic field and homogeneous-heterogeneous reactions on stagnation flow of a casson fluid", Engineering Scince and Technolody, an International Journal 19, 875-887.

Raju,C.S.K., Sandeep, N., Sugunamma,V., Jayachandra Babu,M. & Ramana Reddy, J.V. (2016), ''Heat and Mass transfer in Magnetohydro dynamic Casson fluid over an exponentially permeable stretching surface", Engineering Science and Technology, an Internationa Journal 19, 45-52.

Ramana Reddy,J.V., Sugunamma,V. & Sanddep, N. (2016), "Effect of Aligned Magnetic Field on Casson Fluid Flow Past a Vertical Oscillating Plate in Porous Medium", Journa of Advanced Physics 5 (4), 295-301.

Sajid,M. & Hayat,T. (2008) , "Influence of thermal radiation on the boundary layer flow due to an exponentially stretching sheet", International Communications in Heat and Mass Transfer 35, 347-356.

Shehzad,S.A., Hayat,T. & Alsaedi,A. (2016), "Three-Dimensional MHD Flow of Casson Fluid in Porous Medium with Heat Generation", Journal of Applied Fluid Mechanics,9(1), 215-223.

Shehzad,S.A., Abdullah,Z., Abbasi,F.M., Hayat,T. & Alsaedi,A. (2016), "Magnetic field effect in three-dimensional flow of an Oldroyd-B nanofluid over a radiative surface", Journal of Magnetism and Magnetic Materials 399, 97-108.

Vijendra Singh. & Shweta Agarwal. (2014), "Heat Transfer for two types of viscoelastic fluid over an exponentially stretching sheet with variable thermal conductivity and radiation in porous medium", Heat

Transfer for Two Types of Viscoelastic Fluid Thermal Science 18(4), 1079-1093.

Appendix

$$m_1=\frac{Sc+\sqrt{Sc^2+4Sc\gamma}}{2},\quad A_1=\frac{\mathrm{Pr}+\sqrt{\mathrm{Pr}^2+4\,\mathrm{Pr}\,F}}{2},\quad A_2=\frac{1+\sqrt{1+4P_1\left(1+\frac{1}{\beta}\right)}}{2\left(1+\frac{1}{\beta}\right)},$$

$$A_3=\frac{Gr}{\left(1+\frac{1}{\beta}\right)A_1^{\,2}-A_1-P_1},\quad A_4=\frac{Gm}{\left(1+\frac{1}{\beta}\right)m_1^{\,2}-m_1-P_1},\quad A_5=A_1+A_2,$$

$$A_6=A_3+A_4,\quad B_1=A_2+m_1,\quad B_2=A_1+m_1,\quad B_3=\frac{\mathrm{Pr}\,A_3^2\left(A_1^2+P_2\right)}{4A_1^2-2A_1-\mathrm{Pr}\,F},$$

$$B_4=\frac{\mathrm{Pr}\,A_6^2\left(A_2^2+P_2\right)}{4A_2^2-2A_2\,\mathrm{Pr}-\mathrm{Pr}\,F},\quad B_5=\frac{2\,\mathrm{Pr}\,A_3A_6\left(A_1A_2+P_2\right)}{A_5^2-A_5\,\mathrm{Pr}-\mathrm{Pr}\,F},\quad B_6=\frac{\mathrm{Pr}\,A_4^2\left(m_1^2+P_2\right)}{4m_1^2-2m_1\,\mathrm{Pr}-\mathrm{Pr}\,F},$$

$$B_7=\frac{2\,\mathrm{Pr}\,A_4A_6\left(A_2m_1+P_2\right)}{B_1^2-B_1\,\mathrm{Pr}-\mathrm{Pr}\,F},\quad B_8=\frac{2\,\mathrm{Pr}\,A_3A_4\left(A_1m_1+P_2\right)}{B_2^2-B_2\,\mathrm{Pr}-\mathrm{Pr}\,F},\quad B_9=B_3+B_4-B_5+B_6-B_7+B_8,$$

$$B_{10}=\frac{GrB_9}{\left(1+\frac{1}{\beta}\right)A_1^2-A_1-P_1},\quad B_{11}=\frac{GrB_3}{4\left(1+\frac{1}{\beta}\right)A_1^2-2A_1-P_1},\quad B_{12}=\frac{GrB_4}{4\left(1+\frac{1}{\beta}\right)A_2^2-2A_2-P_1},$$

$$B_{13}=\frac{GrB_5}{\left(1+\frac{1}{\beta}\right)A_5^2-A_5-P_1},\quad B_{14}=\frac{GrB_6}{4\left(1+\frac{1}{\beta}\right)m_1^2-2m_1-P_1},\quad B_{15}=\frac{GrB_7}{\left(1+\frac{1}{\beta}\right)B_1^2-B_1-P_1},$$

$$B_{16}=\frac{GrB_8}{\left(1+\frac{1}{\beta}\right)B_2^2-B_2-P_1},\quad B_{17}=B_{10}-B_{11}-B_{12}+B_{13}-B_{14}+B_{15}-B_{16},$$